

Arrayed High Efficiency Dual-Integrated Microstructured Semiconductor Neutron Detectors

Steven L. Bellinger, *Member, IEEE*, Ryan G. Fronk, *Member, IEEE*, Douglas S. McGregor, *Member, IEEE*, and Timothy J. Sobering

Abstract – Low-power microstructured semiconductor neutron detector (MSND) devices have long been investigated as a high-efficiency replacement for thin-film diodes for thermal neutron detection. The detector devices were improved by stacking two 1cm^2 devices and integrating their responses together to act as a single diode, increasing detection efficiency to over 42%. The need for larger active area devices has driven further improvement of the technology. A large active area device has been developed by arraying seventy-two 1cm^2 devices together into two 6×6 configurations, dual-stacking them, and integrating their responses together in order to act as a single detector device. The intrinsic thermal neutron detection efficiency was found to be $7.03\pm 0.04\%$. The leakage current of the 36cm^2 device was -42nA at -5V bias and the capacitance was found to be 54pF at -5V bias.

I. INTRODUCTION

THIN-film coated semiconductor diodes offered a means of low power, low cost thermal neutron detection. Geometrical limitations and self-absorption of the reaction products limited the devices to 4-5% intrinsic detection efficiency [32-33]. The technology was improved by etching perforations into the semiconductor volume and backfilling the perforations with a neutron reactive material. This increases absorption efficiency of both incident neutrons as well as the resulting reaction products [1-31]. Recently, two silicon-based MSND devices, backfilled with ^6LiF , were stacked on to one another and integrated to function as a single detector as shown in Fig. 1. In doing this, intrinsic thermal neutron detection efficiency was increased to $42\pm 0.25\%$ [32]. This high efficiency has allowed these detectors to better compete with other types of thermal neutron detectors. However, their small active area, currently at 1cm^2 , limits the devices to certain applications. In order to replace other expensive technology, the active detector area of the devices needed to be increased. Unfortunately, as the active area of a semiconductor diode is increased, the leakage current and capacitance of the device also increases. This increases noise and reduces the overall pulse-height produced by the device and therefore reduces the ability to resolve out the signal from the reaction products of a neutron capture event.

Manuscript received November 15, 2011. This work was supported in part by the Defense Threat Reduction Agency under Contract No. DTRA-01-02-D-0067.

Steven L. Bellinger, Ryan G. Fronk, and Douglas McGregor are with the Semiconductor Materials and Radiological Technologies (S.M.A.R.T.) Laboratory, Kansas State University, Manhattan, KS 66506 USA (telephone: 1-785-532-7087, e-mail: rfronk@ksu.edu).

Timothy J. Sobering is with the Electronics Design Laboratory (EDL), Kansas State University, Manhattan, KS 66506 USA.

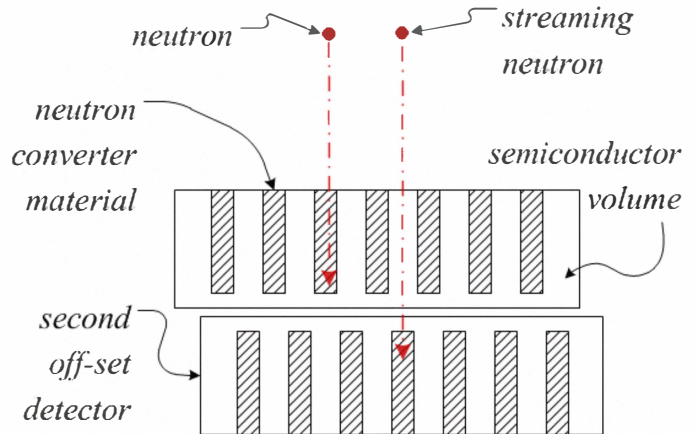


Fig. 1. Illustration of two microstructured devices, backfilled with neutron reactive material, stacked together and integrated to function as a single device. The two devices are off-set slightly in order to reduce neutron streaming. If a neutron is incident on the detector volume on the first detector, the low cross-section of the silicon ($\sigma_{\text{Si,T}}=2.161\text{ b}$) will stream the neutron to the second detector.

Another means of increasing the active area of a semiconductor diode were investigated. A new design used seventy-two 1cm^2 MSND devices arrayed together into two 6×6 arrays. The two devices were then stacked onto one another and offset so as to reduce streaming of thermal neutrons through the trench sidewalls. It is important that both of the 6×6 MSND devices used in this detector produce uniform thermal neutron responses, therefore, great care was taken to ensure that the manufacturing process of the two 6×6 array devices were constant. The two 6×6 arrays were manufactured on two 4-inch n-type silicon wafers and the trenches were etched with a chemical wet-etching technique. The 6×6 array devices were tested for their leakage current and capacitance by plotting their I-V and C-V curves respectively. The devices were then back-filled with ^6LiF and mounted to their electronics.

The assembled array device was tested for its thermal neutron response, fast neutron response, and its gamma-ray rejection capability. For each test, the detector array was compared to a calibrated ^3He gas-filled thermal neutron detector.

II. DEVICE FABRICATION

The arrayed 6×6 1cm^2 MSND devices were fabricated on two separate 100mm wafers with a resistivity of $7\text{-}14\text{k}\Omega\text{-cm}$ and (110) orientation. A silicon dioxide layer was thermally

grown and then etched to form diffusion windows as depicted in Fig. 2. Both wafers were patterned with the same straight trench design using AZ photoresist. The remaining silicon dioxide was etched away with BOE to reveal the bare silicon that was to be etched into trenches. 60 μm -deep, 25 μm -wide trenches were etched along the $\langle 111 \rangle$ plane with a pitch of 50 μm using a potassium hydroxide wet-etching technique. The batch processing capability of the wet-etching technique allowed for both wafers to be etched at the same time, which provided uniform etch characteristics across both wafers. This helped to ensure that their neutron absorption and reaction product responses were similar. The devices were then harvested, cleaned, and then diced into their 36 cm^2 form pictured in Fig. 3. The devices were then conformally diffused with a p-type boron dopant to form the pn -junction. Silicon dioxide was used as the barrier material between diodes. A Ti-Al ohmic contact was evaporated onto the backside to form the cathode of the devices.

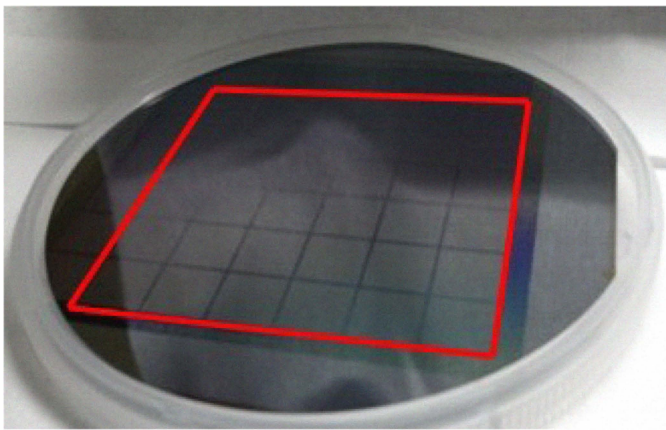


Fig. 2. The 6x6 array device is produced in the same fashion as the individual 1 cm^2 devices previously reported. The diodes are simply left in this configuration and removed from the waste silicon as a single large device. This 6x6 array is then processed as a whole device.

The 6x6 arrays were tested for their diode properties and then backfilled with nano-sized ^6LiF neutron reactive powder material uniformly across the trenches of each of the diodes in the arrays. The arrays were then mounted to the front and back to an aluminum-coated mounting board as pictured in Fig. 3. This mounting board allowed for careful alignment of the two arrays, as shown in Fig. 4., such that the devices worked together to reduce neutron streaming.

In order to reduce the complexity and power consumption of the electronics, the amplifying and pre-amplifying circuits were designed with a unique means of processing counts. Within the 6x6 array of detector diodes, individual diodes were grouped into clusters of four devices. Each of the diodes within this cluster was paired with its own charge sensitive pre-amplifying circuit with a nominal gain of -0.8mV pF^{-1} and a time constant of 10.2 μs . The pre-amplifiers were grouped into clusters of fours on the daughter board as seen in Fig. 4.

Two of these boards were used for the device, one for each MSND device. The pre-amplifier board can be modified to compensate for the DC offset caused by large leakage current from the trenching of the MSND devices.

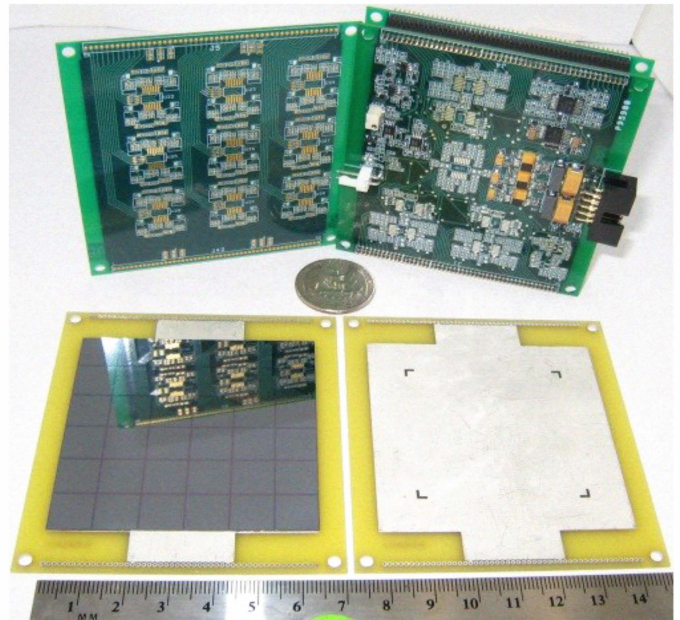


Fig. 3. Image of a 6x6 detector device along with its electronic controller board. The daughter board in the upper left houses the pre-amplifying circuits grouped into nine clusters of four. The mother board houses the amplifying and signal shaping circuits for the detector.

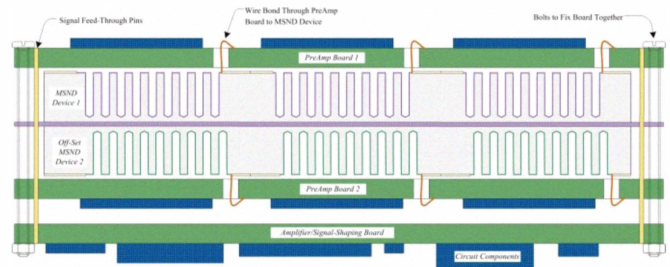


Fig. 4. The two 6x6 MSND devices are stacked, back-to-back between the two pre-amplifier boards. The mother board, which houses the amplifier circuits and shaping circuits are mounted behind the entire assembly. Screws secure the boards together.

The motherboard provides power to and houses the amplifying and pulse-shaping circuits. The supplied power can be varied from a +0V to +2.5V detector bias. The signals from the pre-amplifier boards are routed to the motherboard where it is processed by a pole-zero cancellation stage with a gain of -56 and time constants of 12.1 μs (zero) and 10 μs (pole). An onboard discriminator is capable of outputting a 3.3V logic level when the analog output is above the set LLD, providing a digital output as well as the analog output. The analog output is a semi-Gaussian pulse with a FWHM of 18.5 μs and a gain of 130.2mV/fC. These values were determined using a 100pF detector capacitance. The referred noise is 1.06 fC(rms). During operation, the device requires only 9mA of current.

III. DEVICE TESTING AND RESULTS

The arrayed high-efficiency dual-integrated MSND device neutron-detection efficiency was determined using a mono-energetic 0.0253eV diffraction beam-port located at the TRIGA Mark II nuclear reactor at Kansas State University [34]. This thermal neutron beam is 1.25 cm in diameter. The intrinsic efficiency was determined using a direct comparison method with a calibrated Reuter-Stokes ^3He gas-filled proportional detector [19]. Summed counts from the MSND device and the ^3He filled tube in the 0.0253eV neutron beam are made separately and listed on Table 1.

TABLE I. INTRINSIC THERMAL NEUTRON DETECTION EFFICIENCY

Detector	C.t Time	Counts	Int. Efficiency
Stacked 6x6 ^3He Tube	900 (sec)	51831	7.03 \pm 0.04%
^3He Tube	100 (sec)	67948	80.7% [19]

The intrinsic neutron detection efficiency of the 6x6 array device was found by dividing the summed counts from the array device by the thermal neutron fluence calibrated with the ^3He tube. The LLD of the detector array was set just above system noise with the nuclear reactor off. Expected intrinsic detection efficiency was calculated to be 18.9% [22]. The lower than expected detection efficiency that was found can be explained through various discrepancies between theory, found elsewhere, and this device [22]. The unmicrostructured regions, 0.65mm wide, between the elements of the array are not active regions and thus allow neutron streaming. Also, during the diffusion process, current equipment limitations allow only for a 3-inch diameter portion of the array to be properly diffused, leaving elements on the outside of the array less-functional. However, these factors would only contribute a few-percent deviation from the expected value. Upon further investigation, it was found that a quadrant of the rear facing detector array was not functioning properly, rendering that section of the detector dead. Because detection efficiency was tested in the 1.25cm mono-energetic beam port, correcting the non-functioning region would effectively double the detection

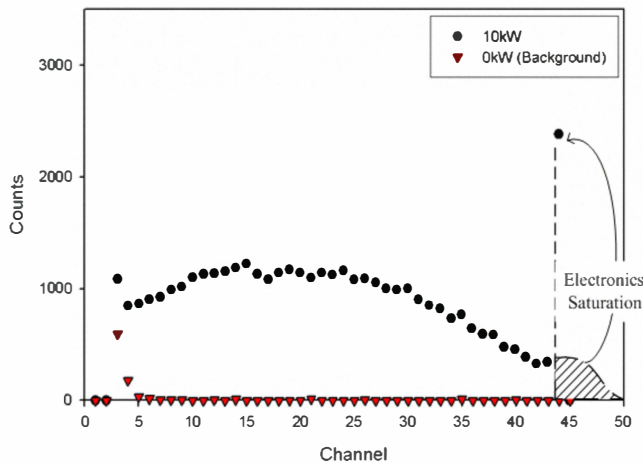


Fig. 5. The reaction produce response spectrum from of the 6x6 array device while exposed to a mono-energetic 0.0253eV neutron beam. The last channel is the electronics saturation channel which houses any event that deposits more energy than that channel.

efficiency. The reaction product response spectrum can be found in Fig. 5.

With thermal neutron sensitivity established, the device was tested to determine the uniformity of the response of all of the elements of the array functioning together. This was accomplished using a ^{252}Cf spontaneous fission neutron source at a distance of 55 cm from the detector. The ^{252}Cf source had a strength of 1.14×10^7 neutrons per second. A lead shield was used to discriminate out any possible gamma-ray emissions from the source. The reaction product response spectrum for the ^{252}Cf test can be found below in Fig. 6.

The 6x6 array device was also tested for its gamma-ray rejection capability using a high-activity ^{137}Cs 662-keV gamma-ray source. At the time of testing, the calibrated source had an activity of 71.74mCi. The device's response was determined at a distance of 55 cm from the source. The gamma-ray response spectrum for the device can be found in Fig. 7.

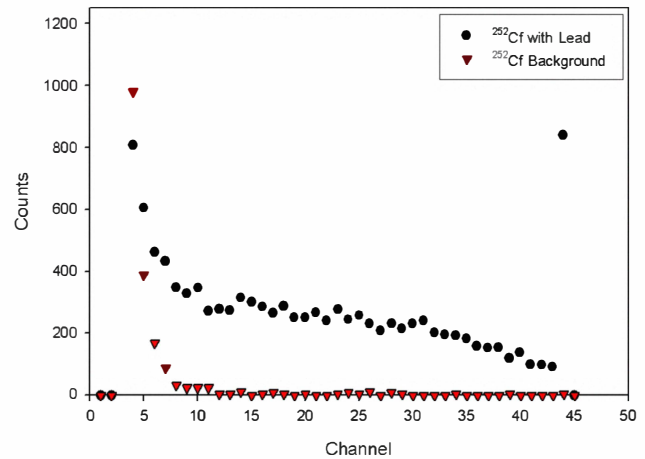


Fig. 6. Pictured is the reaction product response spectrum from of the 6x6 array device while exposed to a ^{252}Cf spontaneous fission neutron source with a Watt energy distribution. The last channel is the electronics saturation channel which houses any event that deposits more energy than that channel.

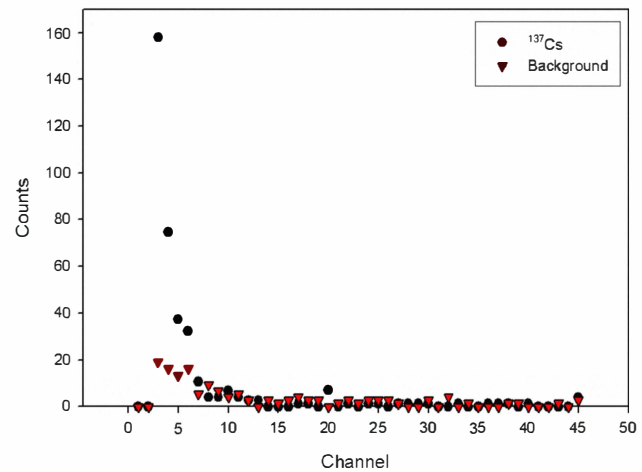


Fig. 7. The response spectrum of incident 662-keV gamma-rays from a ^{137}Cs is pictured with background. It should be noted that this test occurred within the nuclear reactor bay at Kansas State University and that stray neutrons caused counts in the upper channels.

IV. CONCLUSION

The 6x6 arrayed MSND device functioned well as a larger area solid-state neutron detector. The functioning portion of the seventy-two diodes worked together to form a uniform neutron response. Improvements to the MSND devices used for the array and correction of the pre-amplifying circuit board would greatly improve the detector efficiency and neutron response spectrum. With deeper etched trenches and more care to the pitch-to-wall thickness ratio, much greater detection efficiencies can be obtained. Utilization of new diffusion furnaces capable of processing up to 6-inch wafers will help to produce more uniform diffusion of the diodes that will lead to a more uniform neutron response from the diodes during irradiation of the entire detector.

The devices also have the capability to be tiled together to function as an even larger panel array type detector. This capability will be tested as more prototype devices are produced in the coming months.

V. ACKNOWLEDGEMENTS

This work was supported in part by DTRA Contract DTRA01-02-D-0067.

REFERENCES

- [1] D.S. McGregor, M.D. Hammig, H.K. Gersch, Y-H.Yang, and R.T. Klann, "Design Considerations for Thin Film Coated Semiconductor Thermal Neutron Detectors, Part I: Basics Regarding Alpha Particle Emitting Neutron Reactive Films," *Nucl. Instrum. and Meth.*, **A500**, pp. 272-308, 2003.
- [2] D.S. McGregor and J.K. Shultis, "Spectral identification of thin-film-coated and solid-form semiconductor neutron detectors," *Nucl. Instrum. and Meth.*, **A517**, pp. 180-188, 2003.
- [3] C.P. Allier, *Micromachined Si-well Scintillator Pixel Detectors*. Netherlands: DUP Science, 2001.
- [4] D.S. McGregor et al., "New Surface Morphology for Low Stress Thin-Film-Coated Thermal-neutron Detectors," *IEEE Trans. Nucl. Sci.*, **NS-49**, pp. 1999-2004, 2002.
- [5] D.S. McGregor and R.T. Klann, "Pocked Surface Neutron Detector," US-6545281, allowed April 8, 2003.
- [6] J.K. Shultis and D.S. McGregor, "Efficiencies of Coated and Perforated Semiconductor Neutron Detectors," *IEEE Nucl. Sci. Symp. Conf. Rec.*, Rome, Italy, Oct. 16- 22, 2004, pp. 4569-4574.
- [7] J.K. Shultis and D.S. McGregor, "Efficiencies of Coated and Perforated Semiconductor Neutron Detectors," *IEEE Trans. on Nuclear Science*, **NS-53**, pp. 1659-1665, 2006.
- [8] W.J. McNeil et al., "Development of Perforated Si Diodes for Neutron Detection," *IEEE Nucl. Sci. Symp. Conf. Rec.*, San Diego, CA, Oct. 29 – Nov. 5, 2006, pp. 3732-3735.
- [9] D.S. McGregor and R.T. Klann, "High-Efficiency Neutron Detectors and Methods of Making the Same," US-7,164,138, allowed January 16, 2007.
- [10] S.L. Bellinger, W.J. McNeil, T.C. Unruh, and D.S. McGregor, "Angular Response of Perforated Silicon Diode High Efficiency Neutron Detectors," *IEEE Nucl. Sci. Symp. Conf. Rec.*, Honolulu, HI, Oct. 26 – Nov. 3, 2007, pp. 1904-1907.
- [11] D.S. McGregor et al., "Perforated Semiconductor Neutron Detector Modules," *Proc. of 32nd Annual GOMACTech Conf.*, Lake Buena Vista, FL, March 19 - 22, 2007.
- [12] R.J. Nikolic et al., "Fabrication of pillar-structured thermal neutron detectors," *IEEE Nucl. Sci. Symp. Conf. Rec.*, Honolulu, HI, Oct. 26 – Nov. 3, 2007, pp. 1577-1580.
- [13] C.J. Solomon, *Analysis and Characterization of Perforated Neutron Detectors*, Kansas State University, Manhattan, KS, M.S. Thesis, 2007.
- [14] C.J. Solomon, J.K. Shultis, W.J. McNeil, B.B. Rice, and D.S. McGregor, "A Hybrid Method for Coupled Neutron-Ion Transport Calculations for ^{10}B and ^6LiF Coated and Perforated Detector Efficiencies," *Nucl. Instrum. and Meth.*, **A580**, pp. 326-330, 2007.
- [15] J. Uher et al., "Characterization of 3D thermal neutron semiconductor detectors," *Nucl. Instrum. and Meth.*, **A576**, pp. 32-37, 2007.
- [16] J.K. Shultis and D.S. McGregor, "Designs for Micro-Structured Semiconductor Neutron Detectors," *Proc. SPIE*, **7079**, pp. 06:1-06:15, 2008.
- [17] D.S. McGregor, S.L. Bellinger, W.J. McNeil, and T.C. Unruh, "Micro-Structured High-Efficiency Semiconductor Neutron Detectors," *2008 IEEE Nucl. Sci. Symp. Conf. Rec.*, Dresden, Germany, Oct. 19 - 25, 2008, pp. 446-448.
- [18] S.L. Bellinger, W.J. McNeil, and D.S. McGregor, "Improved Fabrication Technique for Microstructured Solid-State Neutron Detectors," *Proc. MRS*, **1164**, 2009, pp. 57-65.
- [19] S.L. Bellinger, W.J. McNeil, and D.S. McGregor, "Variant Designs and Characteristics of Improved Microstructured Solid-State Neutron Detectors," *IEEE Nucl. Sci. Symp. Conf. Rec.*, Orlando, FL, Oct. 25 – 31, 2009, pp. 986-989.
- [20] S.L. Bellinger, W.J. McNeil, T.C. Unruh, and D.S. McGregor, "Characteristics of 3D Micro-Structured Semiconductor High Efficiency Neutron Detectors," *IEEE Trans. on Nucl. Sci.*, **56**, 2009, pp. 742-746.
- [21] D.S. McGregor, W.J. McNeil, S.L. Bellinger, T.C. Unruh, and J.K. Shultis, "Microstructured Semiconductor Neutron Detectors," *Nucl. Instrum. and Meth.*, **A608**, pp. 125-131, 2009.
- [22] W.J. McNeil et al., "1-D Array of Perforated Diode Neutron Detectors," *Nucl. Instrum. Meth.*, **A604**, pp. 127-129, 2009.
- [23] W.J. McNeil et al., "1024-Channel Solid State 1-D Pixel Array for Small Angle Neutron Scattering," *IEEE Nucl. Sci. Symp. Conf. Rec.*, Orlando, FL, Oct. 25 – 31, 2009, pp. 2008-2011.
- [24] J.K. Shultis and D.S. McGregor, "Design and Performance Considerations for Perforated Semiconductor Thermal-Neutron Detectors," *Nucl. Instrum. and Meth.*, **A606**, pp. 608-636, 2009.
- [25] Justin Dingley, Yaron Danon, Nicholas LiCausi, Jian-Qiang Lu, and Ishwara B. Bhat, "Directional Response of Microstructure Solid State Thermal Neutron Detectors," *Trans. of the American Nuclear Society and Embedded Topical Meeting Isotopes for Medicine and Industry*, Las Vega, NV, Nov. 7 - 11, 2010, **103**, pp. 1190-1191.
- [26] C.M. Henderson, Q.M. Jahan, W.L. Dunn, J.K. Shultis, and D.S. McGregor, "Characterization of Prototype Perforated Semiconductor Neutron Detectors," *Radiation Physics and Chemistry*, **79**, pp. 144-150, 2010.
- [27] D.S. McGregor and J.K. Shultis, "Reporting Detection Efficiency for Semiconductor Neutron Detectors; a Need for a Standard," *Nucl. Instrum. and Meth.*, 2011, pp. 167-174.
- [28] W.J. McNeil, *Perforated Diode Neutron Sensors*, Kansas State University, Manhattan, KS, Ph.D. Thesis, 2010.
- [29] R.J. Nikolic et al., "Nine Element Si-based Pillar Structured Thermal Neutron Detector," *Proc. SPIE*, **7805**, pp. 78050O, 2010.
- [30] C.J. Solomon, J.K. Shultis, and D.S. McGregor, "Reduced Efficiency Variation in Perforated Neutron Detectors with Sinusoidal Trench Design," *Nucl. Instrum. and Meth.*, **A618**, pp. 260-265, 2010.
- [31] S.L. Bellinger, R.G. Fronk, W.J. McNeil, T.J. Sobering, and D.S. McGregor, "Enhanced Variant Designs and Characteristics of the Microstructured Solid-State Neutron Detector," *Nucl. Instr. and Meth.*, 2010, in Press.
- [32] S.L. Bellinger et al., "Characteristics of the Stacked Microstructured Solid-State Neutron Detector," *SPIE proc.*, **7805**, pp. 78050N, 2010.
- [33] S.L. Bellinger, R.F. Fronk, W.J. McNeil, T.J. Sobering, and D.S. McGregor, "High Efficiency Dual-Integrated Stacked Microstructured Solid-State Neutron Detectors," *IEEE Nucl. Sci. Symp. Conf. Rec.*, Knoxville, TN, Oct. 30 – Nov. 6, 2010.
- [34] T.C. Unruh, *Development of a Neutron Diffraction System and Neutron Imaging System for Beamport Characterization*, Kansas State University, Manhattan, KS, M.S. Thesis, 2009.